

6th and 8th Order Hermite Integrator for N -body Simulations

Keigo Nitadori^a Junichiro Makino^b

^a*Department of Astronomy, University of Tokyo, 7-3-1 Hongo, Bunkyo-ku, Tokyo 113-0033, Japan*

^b*National Astronomical Observatory of Japan, Mitaka, Tokyo, 181-8588, Japan*

Abstract

We present sixth- and eighth-order Hermite integrators for astrophysical N -body simulations, which use the derivatives of accelerations up to second order (*snap*) and third order (*crackle*). These schemes do not require previous values for the corrector, and require only one previous value to construct the predictor. Thus, they are fairly easy to implement. The additional cost of the calculation of the higher order derivatives is not very high. Even for the eighth-order scheme, the number of floating-point operations for force calculation is only about two times larger than that for traditional fourth-order Hermite scheme. The sixth order scheme is better than the traditional fourth order scheme for most cases. When the required accuracy is very high, the eighth-order one is the best. These high-order schemes have several practical advantages. For example, they allow a larger number of particles to be integrated in parallel than the fourth-order scheme does, resulting in higher execution efficiency in both general-purpose parallel computers and GRAPE systems.

Key words: Methods: N -body simulations, Stellar dynamics

PACS: 95.10.ce, 98.10.+z

1 Introduction

Aarseth (1963) introduced what is now called the “Aarseth scheme” or “the standard scheme” for the direct integration of gravitational N -body systems. It is a combination of the individual timestep algorithm, which allows individual particles to have their own times and timesteps, and variable-stepsizes fourth-order Adams-Moulton predictor-corrector scheme.

The basic idea of individual timestep scheme is as follows. When particle i is integrated from its time t_i to its new time $t_i + \Delta t_i$, the calculation of acceler-

ation is done only at its new time, and positions of all other particles at that time are “predicted” in some way. Thus, Adams-Moulton predictor-corrector schemes in the PEC (predict-evaluate-correct) mode with variable stepsize are suitable for the individual timestep algorithm, because they require the acceleration calculation only at the end of the timestep. In addition, in the PEC mode, the acceleration can be calculated from predicted variables.

If we do not use the individual timestep algorithm, we can easily change timesteps if we use single-step integration schemes such as Runge-Kutta methods. However, Runge-Kutta schemes cannot be combined with the individual timestep algorithm, because they require the calculation of accelerations in intermediate points. In the case of two particles with different timesteps, in order to integrate the particle with longer timestep, we need the position of the other particle in the past. However, with usual implementation of the individual timestep algorithm, such past data is not available. In principle, we could keep the past trajectory of particles as demonstrated by Makino et al. (2006). Such schemes are not yet widely used, though a sample implementation does exist (Hut & Makino, 2007).

The fourth-order Aarseth scheme had been the method of choice for the time integration of gravitational N -body systems. However, the optimal value for the order of the integration scheme has not been known. Makino (1991a) implemented the Aarseth scheme with an arbitrary order, and performed a systematic test of the accuracy. He found that the optimal choice of the order weekly depends on the required accuracy, and if the required accuracy is very high orders higher than 4 would give better results. However, he also found that the fourth-order scheme is close to optimal for practical values of required accuracy. His result, however, is for a pure individual timestep algorithm, for which the calculation cost of the acceleration depends on the order of the integrator, through the calculation cost of predictors for particles other than that integrated. McMillan (1986) and later Makino (1991b) introduced the so-called blockstep scheme, in which the timesteps of particles are quantized to powers of two so that multiple particles share exactly the same time. With this blockstep scheme, the calculation cost of predictors becomes much smaller than that of the force calculation for any practical value of the order of the integration scheme, and therefore high-order schemes become more efficient than in the case of the original individual timestep algorithm.

Makino (1991a) also introduced the concept of Hermite scheme, in which the first time derivative of the acceleration is directly calculated and used to construct the interpolation (actually the extrapolation for the predictor) polynomial. As discussed in Makino & Aarseth (1992), the fourth-order Hermite scheme has an extra advantage that it is quite simple to implement. The predictor polynomial for fourth-order schemes must be at least third order for position and second order for velocity. Fortunately, the directly calculated first

time derivative of the acceleration (*jerk*) is just sufficient to construct predictors. In other words, fourth-order Hermite scheme is effectively a single-step algorithm which does not require the memory of previous timesteps.

Another advantage of the fourth-order Hermite scheme is that it is time-symmetric, when used with the correct-to-convergence mode. This feature has been used to achieve effective time-symmetry for the integration of internal motions of binaries (Funato et al., 1997) or nearly-circular orbits of planetesimals (Kokubo et al., 1998). Also, in (Hut & Makino, 2007), a time-symmetric individual timestep algorithm with Hermite scheme have been implemented.

The calculation cost of the Hermite scheme per timestep is somewhat higher than that of the Aarseth scheme, since the jerk must be calculated as well as the acceleration. However, roughly speaking the Hermite scheme allows the timestep larger than that for the Aarseth scheme by almost a factor of two, while increase in the calculation cost seems to be less than a factor of two. Thus, by switching from the fourth-order Aarseth scheme to the fourth order-Hermite scheme, effective gain in calculation speed is achieved while the calculation program becomes simpler. This combined effect is the reason why the fourth-order Hermite scheme is now widely used.

The result shown in Makino (1991a) implies that for blockstep algorithms higher-order schemes might be more efficient. In this paper, we construct higher-order generalization of the fourth-order Hermite scheme and report their performance.

There are two different ways to construct higher-order generalization of the Hermite scheme. The first one is to use previous timesteps, in the same way as in the original Aarseth scheme. This method was described in Makino (1991a). The other is to use even higher derivatives directly calculated, while still using only two points in time. Of course, it is possible to combine these two methods.

To our knowledge, there have been no published work on the latter approach combined with the individual timestep algorithm. At first sight, it looks non-trivial to combine the direct calculation of the higher-order derivatives and individual timestep algorithm. In section 2, we show that the combination is actually possible and that it is not much difficult compared to the original fourth-order Hermite scheme. In section 3, we present the result of numerical experiments, and section 4 is for discussions.

2 Sixth- and Eighth-Order Hermite scheme

2.1 Basic structure of individual timestep scheme

In the individual timestep scheme, particle i has its own time (t_i), timestep (Δt_i), position (\mathbf{x}_i) and velocity (\mathbf{v}_i) at time t_i , and acceleration (\mathbf{a}_i) and time derivative(s) of acceleration ($\dot{\mathbf{a}}_i, \ddot{\mathbf{a}}_i, \dots$) calculated at time t_i . The integration proceeds according to the following steps:

- (1) Select particle i with a minimum $t_i + \Delta t_i$. Set the global time (t) to be this minimum, $t_i + \Delta t_i$.
- (2) Predict the positions and necessary time derivatives of all particles at time t using the predictor polynomials.
- (3) Calculate the acceleration and its time derivative(s) for particle i at time t , using the predicted positions etc.
- (4) Construct higher order time derivatives using the Hermite interpolation based on the new values of acceleration and its derivatives at time $t_i + \Delta t_i$ and those at the previous time t_i . Apply the corrector to position and velocity using these high-order time derivatives, determine new timestep Δt_i , and update time t_i .
- (5) Go back to step (1).

The above description is for the original individual timestep algorithm, and we usually use the so-called blockstep algorithms, in which the timesteps are quantized to powers of two so that particles of the same stepsize share exactly the same time (McMillan 1986). In this way, we can calculate forces on these particles in parallel.

In the following, we present the force calculation formula, predictor, corrector, timestep criterion and initialization procedure, in this order.

2.2 Direct calculation of higher order derivatives

The gravitational force from particle j to particle i and its first three time derivatives are expressed as

Table 1

Number of floating-point operations in force calculation up to potential, acceleration, jerk, snap and crackle.

Max derivative	Total operations	Operation count
Potential	7 add/sub, 4 mul, 1 div, 1 sqrt	31
Acceleration	10 add/sub, 8 mul, 1 div, 1 sqrt	38
Jerk	21 add/sub, 19 mul, 1 div, 1 sqrt	60
Snap	39 add/sub, 38 mul, 1 div, 1 sqrt	97
Crackle	61 add/sub, 63 mul, 1 div, 1 sqrt	144

$$\mathbf{A}_{ij} = m_j \frac{\mathbf{r}_{ij}}{r_{ij}^3}, \quad (1)$$

$$\mathbf{J}_{ij} = m_j \frac{\mathbf{v}_{ij}}{r_{ij}^3} - 3\alpha \mathbf{A}_{ij}, \quad (2)$$

$$\mathbf{S}_{ij} = m_j \frac{\mathbf{a}_{ij}}{r_{ij}^3} - 6\alpha \mathbf{J}_{ij} - 3\beta \mathbf{A}_{ij}, \quad (3)$$

$$\mathbf{C}_{ij} = m_j \frac{\dot{\mathbf{j}}_{ij}}{r_{ij}^3} - 9\alpha \mathbf{S}_{ij} - 9\beta \mathbf{J}_{ij} - 3\gamma \mathbf{A}_{ij}. \quad (4)$$

Here, we call the first four time derivatives of the acceleration *jerk*, *snap*, *crackle* and *pop*, and α , β and γ are given by

$$\alpha = \frac{\mathbf{r}_{ij} \cdot \mathbf{v}_{ij}}{r_{ij}^2}, \quad (5)$$

$$\beta = \frac{|\mathbf{v}_{ij}|^2 + \mathbf{r}_{ij} \cdot \mathbf{a}_{ij}}{r_{ij}^2} + \alpha^2, \quad (6)$$

$$\gamma = \frac{3\mathbf{v}_{ij} \cdot \mathbf{a}_{ij} + \mathbf{r}_{ij} \cdot \dot{\mathbf{j}}_{ij}}{r_{ij}^2} + \alpha(3\beta - 4\alpha^2), \quad (7)$$

where \mathbf{r}_i , \mathbf{v}_i , \mathbf{a}_i , $\dot{\mathbf{j}}_i$ and m_i are the position, velocity, total acceleration, total jerk and mass of particle i , and $\mathbf{r}_{ij} = \mathbf{r}_j - \mathbf{r}_i$, $\mathbf{v}_{ij} = \mathbf{v}_j - \mathbf{v}_i$, $\mathbf{a}_{ij} = \mathbf{a}_j - \mathbf{a}_i$ and $\dot{\mathbf{j}}_{ij} = \dot{\mathbf{j}}_j - \dot{\mathbf{j}}_i$ (Aarseth, 2003).

Table 1 shows the number of floating point operations needed to calculate the terms from potential to crackle. We used the conversion factor 20 for the operation counts for one division and one square root operations, following the convention introduced by Warren et al. (1997). Compared to the calculation up to jerk, the increase of the operation count for higher order terms is rather modest. Even the calculation up to crackle is only about a factor of two more expensive than that up to jerk. Thus, if the eighth-order scheme allows two times larger timestep than that for fourth order scheme for the same accuracy, the eighth-order scheme is more efficient. Of course, the CPU time is not

directly proportional to the number of floating point operations, and therefore the actual efficiency might be somewhat different.

2.3 The necessary orders of predictor and corrector

In the case of fourth-order Hermite scheme, we used two points in time and acceleration \mathbf{a} and jerk \mathbf{j} . To construct a sixth-order scheme, we need to add one more term, snap \mathbf{s} , to the corrector. With two evaluations, at the beginning and at the end of the timestep, of the three variables \mathbf{a} , \mathbf{j} and \mathbf{s} , we indeed have the six values needed for a sixth-order scheme.

One practical question is how to construct the predictor. In the case of the fourth-order scheme, it is sufficient to use the terms up to jerk, since the leading error of the predicted position then becomes $O(\Delta t^4)$, which is consistent with the order of the integrator (Aarseth 1963). In the case of the sixth-order scheme, we need the predictor with terms up to crackle (third derivative of the acceleration), to be consistent. On the other hand, the corrector requires terms only up to snap. Therefore, we directly calculate the derivatives only up to snap, and evaluate the crackle using Hermite interpolation. The interpolation formula for crackle, as well as those for fifth and sixth-order terms, are given in Appendix A.1. Those for the eighth-order scheme are given in Appendix A.2.

2.4 Predictor

The predictor for the sixth-order integrator is given by

$$\mathbf{r}_{i,p} = \mathbf{r}_i + \mathbf{v}_i \Delta t + \frac{1}{2} \mathbf{a}_i \Delta t^2 + \frac{1}{6} \mathbf{j}_i \Delta t^3 + \frac{1}{24} \mathbf{s}_i \Delta t^4 + \frac{1}{120} \mathbf{c}_i \Delta t^5, \quad (8)$$

$$\mathbf{v}_{i,p} = \mathbf{v}_i + \mathbf{a}_i \Delta t + \frac{1}{2} \mathbf{j}_i \Delta t^2 + \frac{1}{6} \mathbf{s}_i \Delta t^3 + \frac{1}{24} \mathbf{c}_i \Delta t^4, \quad (9)$$

$$\mathbf{a}_{i,p} = \mathbf{a}_i + \mathbf{j}_i \Delta t + \frac{1}{2} \mathbf{s}_i \Delta t^2 + \frac{1}{6} \mathbf{c}_i \Delta t^3. \quad (10)$$

Note that we need to predict acceleration, since it is used to calculate snap (see equation 3). For eighth-order scheme, we need to include two additional terms for each predictor, and we also need to predict jerk. Since the predictor is simply a Taylor expansion, we do not give the specific forms for the eighth-order scheme here.

2.5 Corrector

The sixth-order corrector is given by

$$\mathbf{v}_{i,c} = \mathbf{v}_{i,0} + \frac{\Delta t}{2}(\mathbf{a}_{i,1} + \mathbf{a}_{i,0}) - \frac{\Delta t^2}{10}(\mathbf{j}_{i,1} - \mathbf{j}_{i,0}) + \frac{\Delta t^3}{120}(\mathbf{s}_{i,1} + \mathbf{s}_{i,0}), \quad (11)$$

$$\mathbf{r}_{i,c} = \mathbf{r}_{i,0} + \frac{\Delta t}{2}(\mathbf{v}_{i,c} + \mathbf{v}_{i,0}) - \frac{\Delta t^2}{10}(\mathbf{a}_{i,1} - \mathbf{a}_{i,0}) + \frac{\Delta t^3}{120}(\mathbf{j}_{i,1} + \mathbf{j}_{i,0}). \quad (12)$$

See Appendix A.1 for the details of derivation. Note that we gave the simplest form for the corrector of the position, which uses jerks but not snaps. It is possible to construct the corrector which use the snaps, but that would not change the order of the time integration. For special problems such as integration of near-Kepler orbit with constant timestep, appropriate treatment of this highest-order term improves the behavior of the integrator (Kokubo & Makino, 2004).

The eighth-order corrector is given by

$$\begin{aligned} \mathbf{v}_{i,c} = & \mathbf{v}_{i,0} + \frac{\Delta t}{2}(\mathbf{a}_{i,1} + \mathbf{a}_{i,0}) - \frac{3\Delta t^2}{28}(\mathbf{j}_{i,1} - \mathbf{j}_{i,0}) \\ & + \frac{\Delta t^3}{84}(\mathbf{s}_{i,1} + \mathbf{s}_{i,0}) - \frac{\Delta t^4}{1680}(\mathbf{c}_{i,1} - \mathbf{c}_{i,0}), \end{aligned} \quad (13)$$

$$\begin{aligned} \mathbf{r}_{i,c} = & \mathbf{r}_{i,0} + \frac{\Delta t}{2}(\mathbf{v}_{i,c} + \mathbf{v}_{i,0}) - \frac{3\Delta t^2}{28}(\mathbf{a}_{i,1} - \mathbf{a}_{i,0}) \\ & + \frac{\Delta t^3}{84}(\mathbf{j}_{i,1} + \mathbf{j}_{i,0}) - \frac{\Delta t^4}{1680}(\mathbf{s}_{i,1} - \mathbf{s}_{i,0}). \end{aligned} \quad (14)$$

See A.2 for the details of the derivation.

2.6 Timestep criterion

For a high-order integration scheme with adaptive timestep to work properly, it is essential to use an appropriate timestep criterion. In this paper we consider two different timestep criteria. The first one is the generalization of the ‘‘Aarseth’’ criterion

$$\Delta t = \sqrt{\eta \frac{|\mathbf{a}||\mathbf{a}^{(2)}| + |\mathbf{a}^{(1)}|^2}{|\mathbf{a}^{(1)}||\mathbf{a}^{(3)}| + |\mathbf{a}^{(2)}|^2}}, \quad (15)$$

where $\mathbf{a}^{(k)}$ is the k th derivative of acceleration and η is a parameter which controls the accuracy. Usually, a value around 0.02 is used for η . This criterion

is known to work well with fourth-order schemes, but it is also known that it works well only with fourth-order schemes and does not give good results for higher-order schemes (Makino, 1991a). Aarseth (2003) notes that this criterion should be generalized to include the highest derivative available in higher-order integrators.

We tried to generalize the above criterion to higher-orders as

$$\Delta t = \eta \left(\frac{A^{(1)}}{A^{(p-2)}} \right)^{1/(p-3)} \quad (16)$$

where

$$A^{(k)} = \sqrt{|\mathbf{a}^{(k-1)}||\mathbf{a}^{(k+1)}| + |\mathbf{a}^{(k)}|^2}. \quad (17)$$

Here, p is the order of the integrator. We moved the accuracy parameter η out of the fractional power, so that the timestep is directly proportional to η . The numerator is the same as that for the Aarseth criterion for the fourth-order scheme, and for the denominators we used the terms of highest orders available. The fractional power is chosen to give correct dimension of time. This criterion should behave reasonably well, since it does reflect the high-order terms.

We also tested a criterion which is based on the error of the predictor

$$\Delta t_{new} = \Delta t_{old} \left(\frac{\epsilon |\mathbf{a}|}{|\mathbf{a} - \mathbf{a}_p|} \right)^{1/p}, \quad (18)$$

where \mathbf{a}_p is the predicted acceleration and \mathbf{a} is calculated one. In order to use this criterion the acceleration needs to be predicted to the highest order (see section 2.3).

2.7 Initialization

One practical advantage of the fourth-order Hermite scheme is that it is effectively a single-step algorithm and therefore does not need any special initialization procedure, except that the initial timestep must be chosen differently. Unfortunately, this single-step nature is lost when we go to higher orders, since higher derivatives for the predictor need to be constructed using a Hermite interpolation.

The simplest implementation of the initialization procedure is just to use lower-order predictors for the first timestep and use appropriately small timestep. In our current implementation, for the startup of the sixth-order integrator we use the terms up to crackle directly calculated and the Aarseth criterion (15), as was done in the Aarseth code. Thus, the order of the predictor is consistent.

For the eighth-order integrator, we omit the calculation of further derivatives and start with (15) with a small accuracy parameter.

3 Numerical test

In this section, we report the behavior of the sixth- and eighth-order Hermite schemes, for time integration of a 1024-body Plummer model. We used the standard units where the total mass of the system and gravitational constants are both unity and the total energy of the system is $-1/4$. For all calculations, we used a softened gravitational potential with $\varepsilon = 4/N = 1/256$. We used the block timestep algorithm timesteps are restricted to be powers of two, and we set an upper limit of timestep as $1/16$. All calculations were performed in IEEE 754 double precision.

3.1 Result for short-time integration

Figure 1 shows the relation between the maximum relative energy error during the integration for 10 time unit and the average number of timesteps per particle per unit time. To suppress possible effects of the start-up procedure, we first integrate the system for $1/8$ unit time and measured the maximum relative deviation of the energy during the next 10 time units.

We can clearly see that the error of sixth- and eighth-order schemes are proportional to Δt^6 and Δt^8 , as expected. For the relative accuracy of 10^{-8} , the sixth-order scheme allows the average timestep which is almost a factor of three larger than that necessary for the fourth-order scheme. For the relative accuracy of 10^{-11} , the eighth-order scheme allows the average timestep which is about a factor of seven larger than that necessary for the fourth-order scheme. Even for the relatively low accuracy of 10^{-6} , the sixth-order scheme allows about a factor of two larger timestep than the fourth-order scheme does.

Among the three schemes (different predictor orders and different timestep criteria), the difference in the achieved accuracy is not very large, but there are some trends. For example, when we compare the results with low-order predictors and that with high-order predictors, low-order predictors give systematically better results, at least for the fourth order integrators. One possible reason is that the high-order predictor is effectively less time-symmetric compared to low-order predictor, simply because it uses the information from the previous timestep. When we compare two timestep criteria, formula (18) seems to be worse, at least for large stepsizes. Thus, among these three implementations, the combination of low order predictor and generalized Aarseth

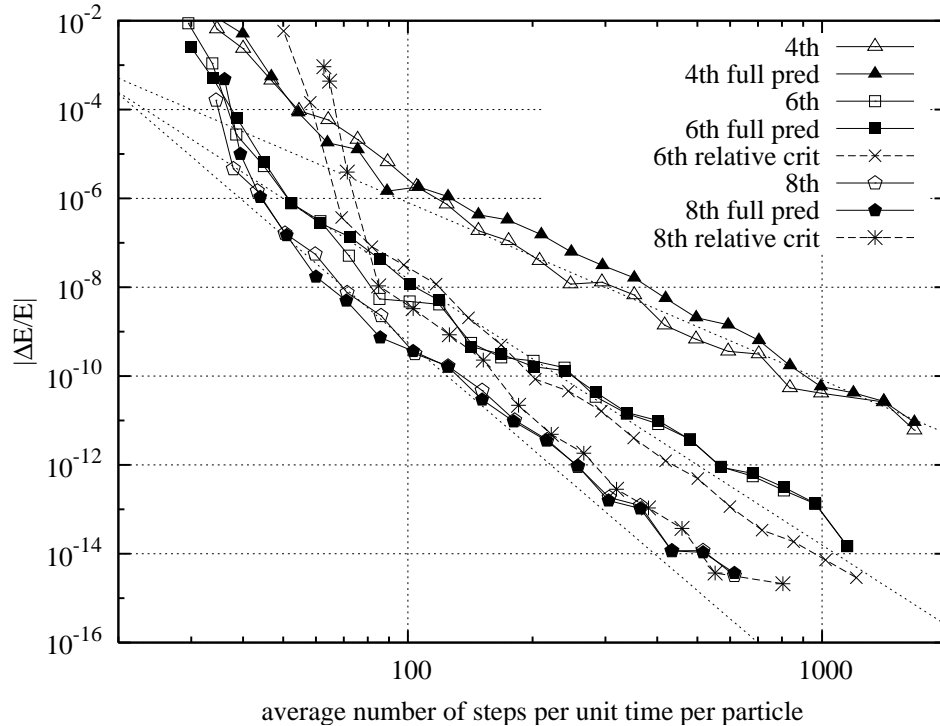


Fig. 1. Maximum relative deviation of the total energy during the time integration for 10 time units, as a function of average number of timesteps per particle per unit time. Triangles, squares and pentagons represent the results of 4th-, 6th- and 8th-order schemes. Open, filled and star-shape symbols indicate the lowest order predictor with generalized Aarseth criterion (16), full high-order predictors with generalized Aarseth criterion, and full high-order predictor with timestep criterion based on the predictor error (18). The three dotted lines indicate the expected scaling relations for 4th-, 6th- and 8th-order algorithms (top to bottom).

criterion seems to be the most safe. It also requires the least amount of floating point operations per timestep.

3.2 Long-term integration

We integrated the system until the core collapse occurs. Since we used a softened potential, a compact core of the size comparable to the softening length is formed after the core collapse. We stopped the calculation at that point. The accuracy parameter was chosen so that the actual CPU time per unit time integration is initially similar. The actual value of the accuracy parameter for the criterion (16) is 0.1, 0.4, and 0.75 for 4, 6 and 8th order schemes.

Notice that the system has a chaotic nature, and even if we start from slightly different two models, the positions of each particle would be completely different after a long-term integration.

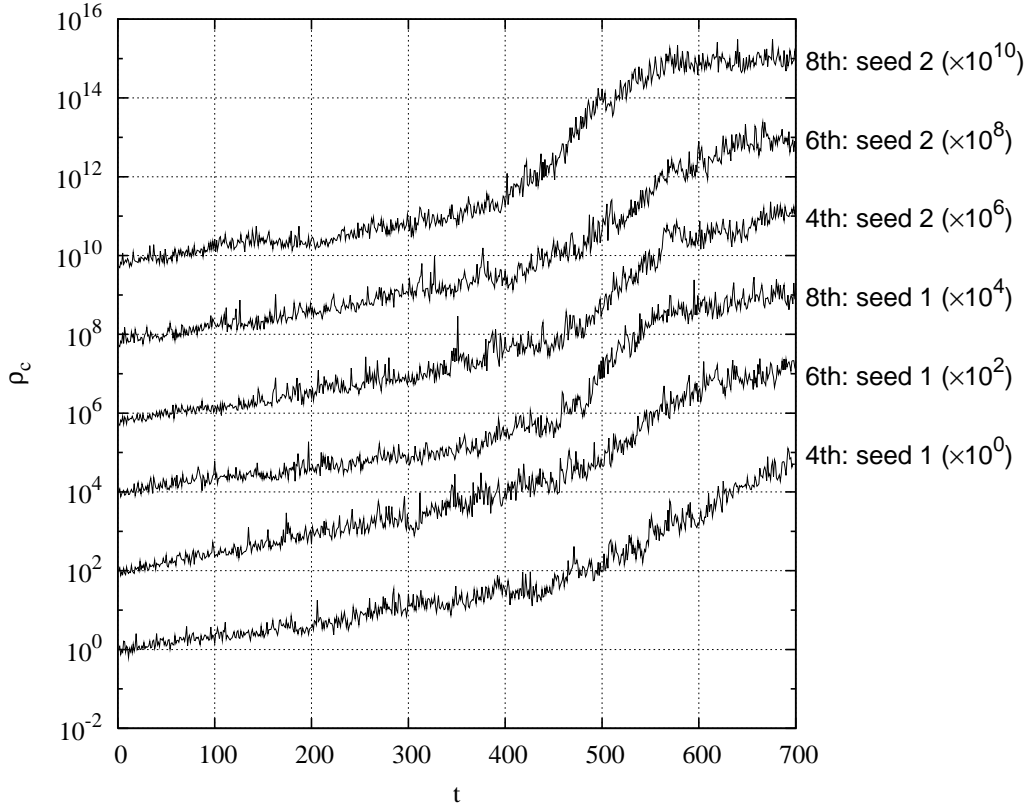


Fig. 2. Time evolution of the central density ρ_c for long-term integrations, for three different integration orders and two different values of the random seed for the initial model. The curves are shifted by factors of 100.

Figure 2 shows the evolution of the central density ρ_c . The overall behavior is similar for all runs. Figure 3 shows the cumulative relative energy error and relative energy error per unit time. As expected, higher-order schemes achieve higher accuracy, though the number of timestep per unit time is smaller. With all schemes, the error per unit time becomes larger as the system evolves. However, this increase is smaller for higher-order schemes. If we compare the error per unit time at the beginning and the end of the calculation, with fourth-order scheme the error at the end is bigger by nearly three orders of magnitude. In the case of the eighth-order scheme, the increase is only around a factor of 10. In the case of the sixth-order scheme, the increase is in between those for fourth- and eighth-order schemes.

This result seems to suggest that the higher-order schemes are actually more robust than the fourth-order scheme. However, it is not clear from where such a difference comes from. Naively, the increase of the integration error is understood as coming from particles in the core, which need to be integrated for a large number of orbits since the orbital timescale is short. Since the structure of the system is not much different, orbital timescales of particles in the core should not depend on the integration schemes used, and there is no reason for the errors to behave differently.

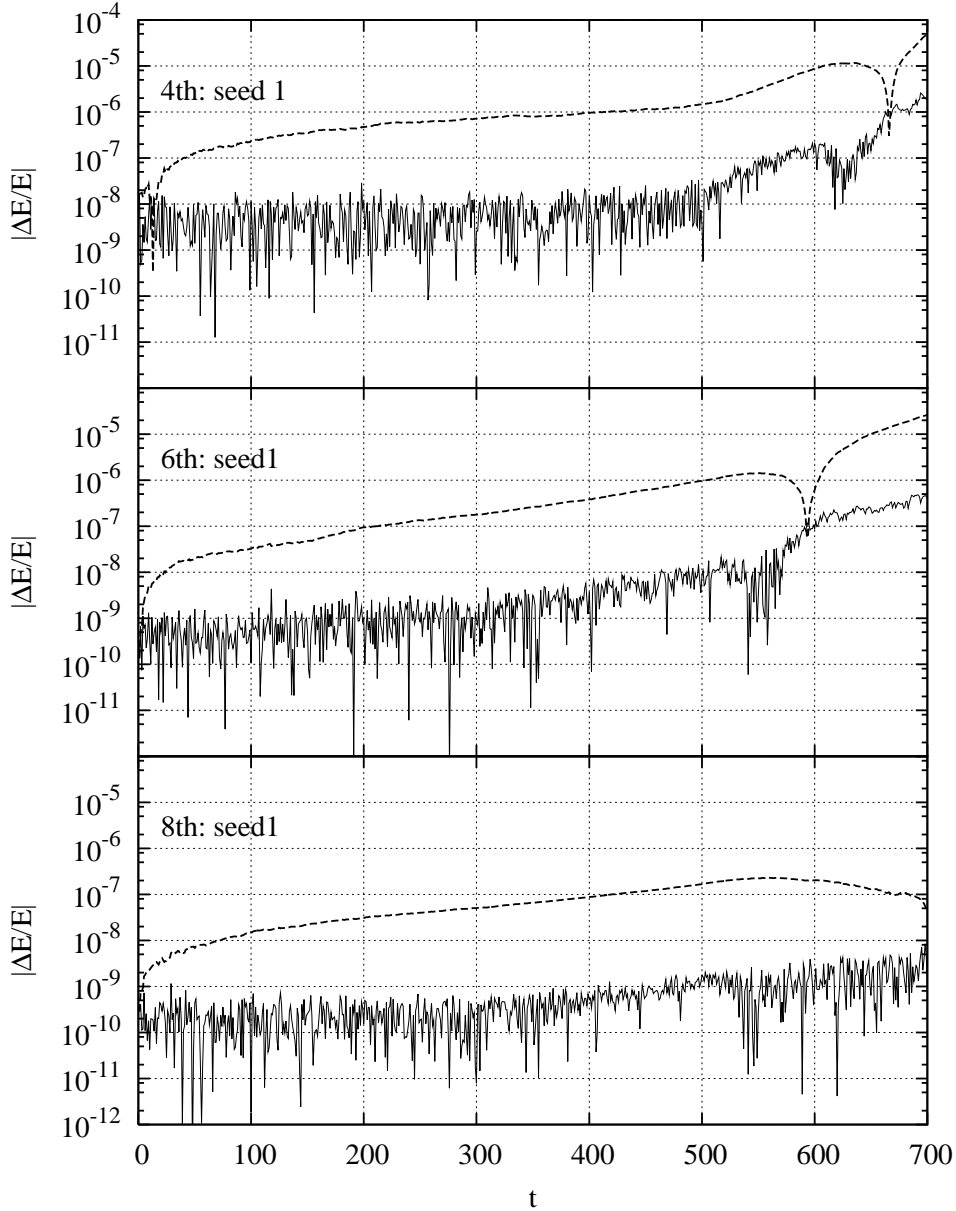


Fig. 3. Total energy error ($|E(t) - E(0)|/|E(0)|$, dashed curve) and energy change in one unit time ($|(E(t) - E(t - 1))|/|E(0)|$, solid curve) in 4th, 6th and 8th order integrators.

Figure 4 shows the average number of timesteps per particles per unit time $\langle n_{steps} \rangle$ (top panel) and the average number of particles integrated in one blockstep $\langle n_b \rangle$ (bottom panel). We can see that the increase in the number of timesteps is the largest for the eighth-order scheme, and this increase in the number of timesteps seems to be the reason for the small error in the later time shown in figure 3. Another notable behavior of the higher-order schemes is that the average number of particles integrated in one blockstep

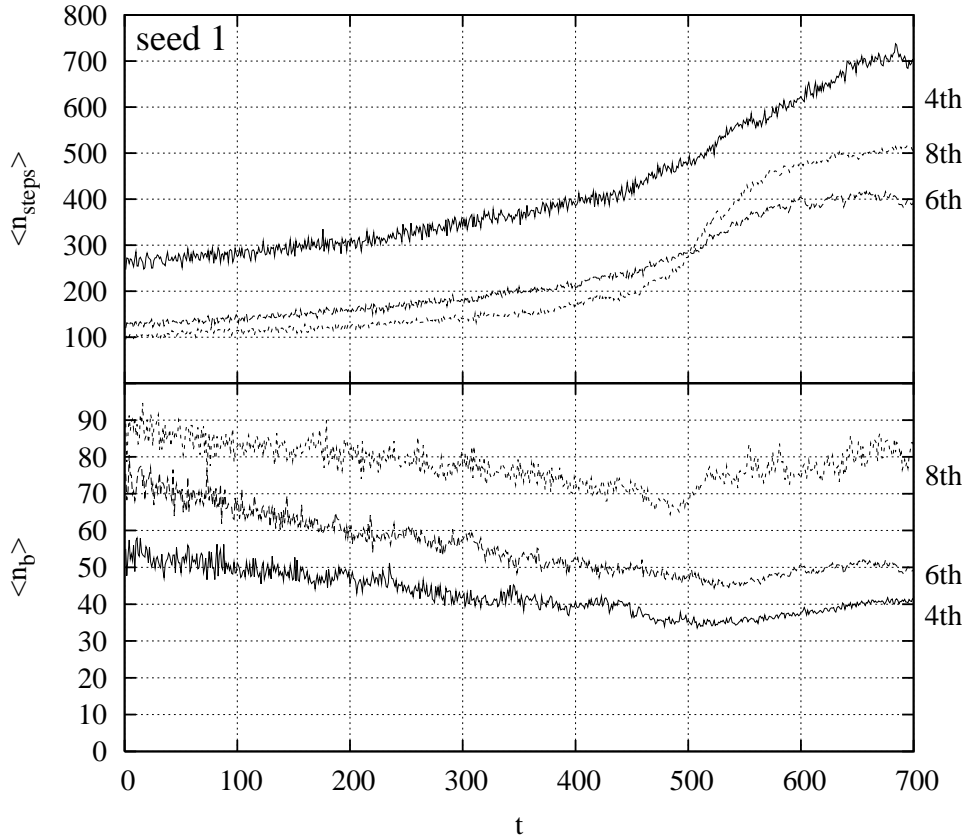


Fig. 4. The average number of steps per particle per unit time $\langle n_{steps} \rangle$ (top) and the average number of particles advanced in one block-step $\langle n_b \rangle$ (bottom).

is larger in higher-order schemes. This means that the timestep criteria for Hermite schemes with different orders respond differently to the change of the structure of the system. In the following, we examine the reason of this behavior of the timesteps.

In order to examine the behavior of the timestep criterion for different orders, it is necessary to calculate the timesteps with different orders for identical distribution of particles. We can of course do this for initial condition, but exact comparison is impossible for the later times. In order to make the comparison, we used the system integrated with the eighth-order scheme, and calculated the timesteps with fourth- and sixth-order criteria using the derivatives obtained by the eighth-order Hermite interpolation. To determine the stepsize, we used the accuracy parameter η same as that used in the actual time integration.

Figure 5 shows the distribution of timesteps for initial Plummer model and after the core collapse ($T = 700$). We can see that the distribution of timesteps depends strongly to the order of the integrator. Even for the initial condi-

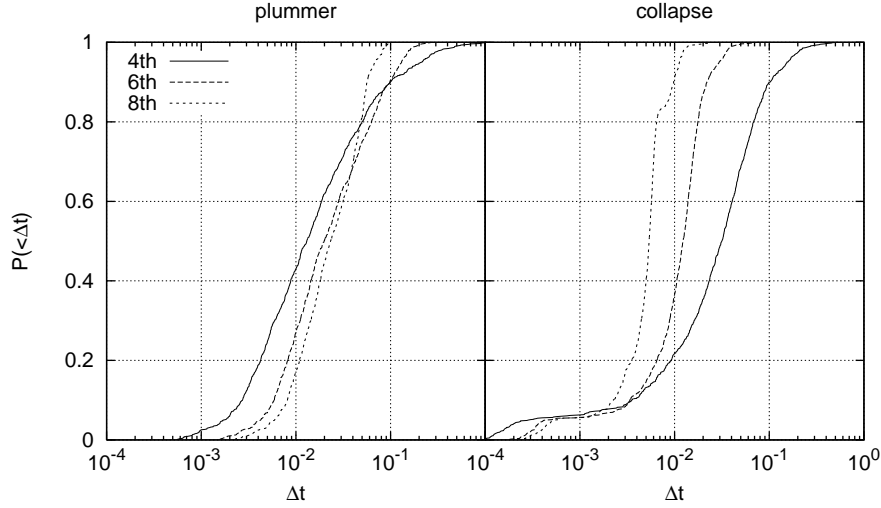


Fig. 5. Cumulative distribution of timestep for the initial Plummer model (left) and that after the core collapse (right). Solid, dashed and dotted curves shows the timesteps calculated with fourth-, sixth-, and eighth-order timestep criteria.

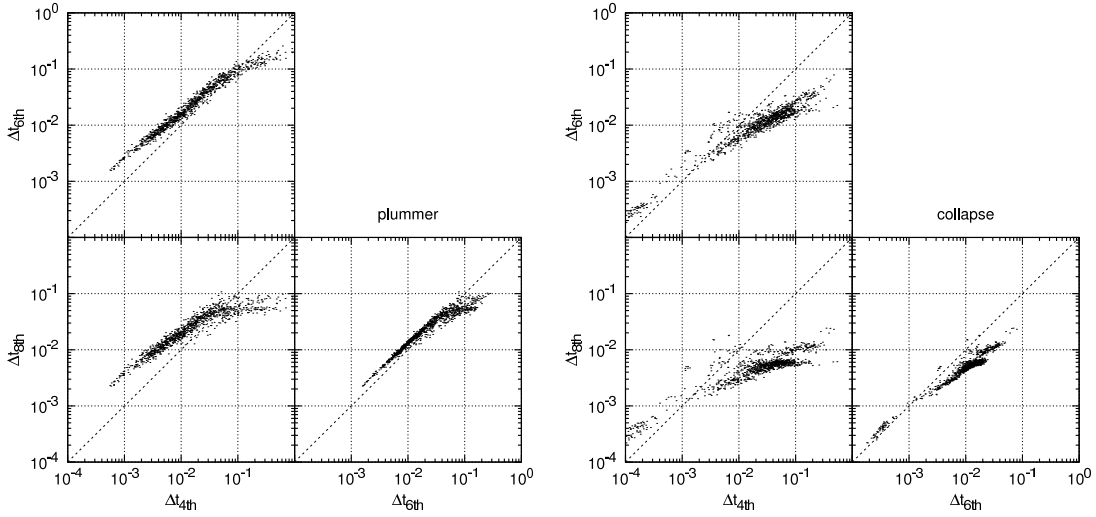


Fig. 6. Relations of timesteps calculated using the timestep criteria for three integrations schemes with orders, for the initial Plummer model (left) and after the core collapse (right). Top-left, bottom-left and bottom-right panels shows the relations between schemes with orders (4-6), (4-8) and (6-8), respectively.

tion, the range of timesteps of particles for the eighth-order scheme is much narrower than that for the fourth-order scheme. This tendency is much more pronounced for the system after the core collapse. Thus, for particles with smallest timesteps, timestep criteria with different orders give similar values. However, particles with large timesteps have very different stepsizes, depending on the order of the timestep criterion.

Figure 6 shows actual values of timesteps calculated using timestep criteria of

different orders as two-dimensional scattergrams. We can see the correlation is quite tight, but at the same time highly nonlinear. While particles with small stepsize (those in the central region of the system) have similar stepsizes when calculated with different orders, particles with large stepsizes (those in the outer region of the system) have very different stepsize depending on the order. In particular, it seems high-order schemes have maximum stepsizes which depend on the structure of the system. The initial Plummer model allows timesteps up to around 0.1, while for the collapsed system timestep cannot significantly exceed 0.01 in the case of the eighth-order scheme. In other words, the timestep of particles far away from the central region of the system somehow shrinks by a factor of 10 in the case of the eighth-order criterion, while no such shrinking is visible for the fourth-order criterion.

3.3 Toy model

In order to understand this behavior, let us consider a simplified model of the collapsed system. Assume that the distribution of particles outside the core is isothermal with $\rho \propto r^{-2}$, and the core size is r_c . Total mass of the system within radius $r = 1$ is 1, and orbital timescale of particles at radius r is r . The mass inside radius r is r for $r_c < r < 1$. The number of particles in $r < 1$ is N and mass of particles m is $1/N$. In these units, The core mass m_c is around r_c , within a factor of two or so.

First, we consider the contribution of the nearest neighbor, for a particle at $r = 1$. The distance to the nearest neighbor is roughly $r_n = 1/N^{1/3}$. The timescale in which this distance changes is also $(r_n/v) = 1/N^{1/3}$, where v is the typical relative velocity and is order unity. Therefore, the acceleration and its k -th derivative have the strength of around

$$|a_n^{(k)}| \sim m r_n^{-2} (r_n/v)^{-k} \sim N^{(k-1)/3}. \quad (19)$$

We can see that the timestep criteria of the form (16) would give similar stepsize of $1/N^{1/3}$ for different orders, if the higher order terms are dominated by the contributions from near neighbors. To put it in words: if you use a local criterion to determine an integration step time scale, you will always get the time needed to reach your nearest neighbor.

Now consider the contribution from one particle at small distance $r \ll 1$ from the center, to a particle at distance one from the center. The strength of the acceleration is of the order $m = 1/N$. The orbital timescale is the larger of r and r_c . We call this value, the larger of r and r_c , as r_* . The timescale of the change of the acceleration Δt is the orbital timescale r_* , and the fractional change in the acceleration is also order r_* : $\Delta a \sim m r_*$. Thus the time

derivatives of the acceleration have the strength of

$$|a_r^{(k)}| \sim \Delta a / (\Delta t)^k \sim m r_* \cdot r_*^{-k} \sim \frac{1}{N r_*^{k-1}} \quad (k > 0). \quad (20)$$

If $r_* < 1/N^{1/3}$, the contribution to the high order derivative of a particle at distance one from the center of the system is larger for a particle with distance $r \leq r_*$ from the center than for the nearest neighbor, for sufficiently large values of k . For our numerical experiment, the size of the core at the core collapse is around 0.003, which is much smaller than $1/N^{1/3}$. Thus, for high enough orders like $k = 7$, it seems natural that the contributions from the particles in the core dominate. For $k = 3$, the nearest neighbor might still be dominant.

From the viewpoint of the accuracy of the time integration, it seems obvious that the behavior of higher order criteria is better. With low-order criteria, we effectively ignore the high-frequency variation of the acceleration when integrating the orbits of particles far away from the core. As a result, there must be the sampling error or aliasing error for the forces from particles in the core, which should show up as the integration error. The energy error of one particle, due to one particle in the core, in one timestep would be of the order of $\Delta E \sim mv\Delta a\Delta t$, since the distance one particle moves in one timestep is $mv\Delta t$ and the force error applied during the time the particle moves is Δa . Thus, we have $\Delta E \sim \Delta t r_c N^{-2}$.

The number of error terms is proportional to the number of particles in the system N , number of particles in the core $r_c N$, and the average number of timesteps per unit time Δt^{-1} . Thus, for one time unit, the total error would be of the order of

$$\Delta E_{\text{sampling}} \sim \sqrt{N \cdot r_c N \cdot \Delta t^{-1} \Delta t r_c N^{-2}} = N^{-1} r_c^{2/3} \Delta t^{1/2}. \quad (21)$$

Here, we assumed that the errors are random and the total error is proportional to the square-root of the number of error terms. Either assumption might not be correct. For example, error terms of the forces on different particles from one particle in the central region are likely to be correlated. Therefore the actual error might be larger.

In the above, we assumed that the error comes only from the sampling of the acceleration. However, with Hermite schemes, what we actually integrate is the high order derivatives directly calculated. Thus, the actual error is probably much bigger than the estimate above. In the case of the fourth-order Hermite scheme which uses the first time derivative, the derivative is of the order $1/N$ from equation (20). Therefore, the energy error of one particles is more like

$\Delta E \sim mv|a_r^{(1)}|\Delta t^2 \sim \Delta t^2 N^{-2}$ per timestep, and total error is of order of

$$\Delta E_{\text{sampling,jerk}} \sim N^{-1} r_c^{1/2} \Delta t^{3/2}. \quad (22)$$

Note that the only way, for the current individual timestep scheme, to make this error reasonably small is to shrink the timestep of *all* particles in the system so that the orbits of core particles are resolved. In that sense, the behavior of the eighth-order scheme is numerically correct, and that of fourth-order scheme is not. This is probably the reason why the error increases for the fourth-order scheme.

4 Discussion

4.1 Computational aspects

In this paper, we present sixth- and eighth-order Hermite schemes to be used with individual timestep algorithm, and compared their performance with that of the fourth-order scheme. We found that these higher-order schemes do offer practical advantages.

Here we speculate on the merit of higher-order schemes, when used with special-purpose computers or parallel implementation of individual timestep algorithm on massively-parallel computers.

One advantage of the direct calculation of higher-order derivatives in hardware is that calculation of higher-order terms can be implemented with short word lengths. In the case of GRAPE-4 (Makino et al., 1997) or GRAPE-6 (Makino et al., 2003), the calculation of acceleration is done with 24-bit mantissa and jerk with 20-bit mantissa. Similarly, it would be okay to calculate snap in 16 bits and crackle in 12 bits. Thus, though the number of operations becomes large as we calculate higher-order terms, the silicon area needed does not increase much. Even in the case of general-purpose programmable computers (including GPUs), higher-order schemes have extra advantage, since the calculation of high-order terms can be done in lower precision, for example single precision. Many of general-purpose CPUs have extra instructions for fast single-precision operations, and GPUs are much faster in single precision than in double precision.

Another advantage is that the number of particles integrated in one blockstep is larger for higher-order schemes. Thus, we can enjoy more parallelism with higher-order schemes, resulting in higher execution efficiency for both general-purpose parallel computers and GRAPEs.

Thus, the higher-order schemes are better not just in the pure operation count but also in hardware efficiency and parallel efficiency.

4.2 Physical/mathematical aspects

In section 3.2, we have seen that, for high-order schemes, timesteps of a particles in outer region of the system become short to resolve the high-frequency variation of the acceleration due to particles in the central region. In the case of low-order schemes, such shrinking did not occur. However, as a result the energy error became very large. Thus, it seems that we need to make the timestep of all particles small, as the system evolves and the core size becomes smaller. This means that the analysis of the calculation cost based on the assumption that the nearest neighbor determines the timestep (Makino & Hut, 1988) is not correct.

Our conclusion implies that the individual timestep algorithm is not so effective as shown in Makino & Hut (1988), because the maximum timestep of particles is larger than that of the shortest timestep by the factor which only weakly depends on the number of particles in the system. In principle, however, we can reduce the calculation cost by assigning individual timesteps not to particles but to interactions. Even when there is a small core with short orbital period, the force between two particles both far away from the core changes smoothly. Strictly speaking, it is not really smooth, since the position and velocity contain the high-frequency terms. However, these high frequency terms are much smaller than that of accelerations simply because position and velocity are obtained by integrating the acceleration. Thus, if we use relatively low-order schemes or the original Adams-type scheme which does not use the time derivatives, we might be able to integrate the interaction between two particles far away from the core with the timestep much larger than that of core particles. We will investigate the possibility of such a scheme in future papers.

We thank Sverre Aarseth for his lectures and discussions at Mitaka on November, 2007. K. N. is financially supported by Research Fellowship of the Japan Society for the Promotion of Science (JSPS) for Young Scientists. This work was supported in part by the Special Coordination Fund for Promoting Science and Technology (GRAPE-DR project), from the Ministry of Education, Culture, Sports, Science and Technology (MEXT) of Japan.

A Notes for implementers

A.1 Interpolation polynomial for the sixth-order integrator

We consider constructing an interpolation polynomial from acceleration, jerk and snap at time t_0 , (a_0, j_0, s_0) and those at t_1 , (a_1, j_1, s_1) . We define summations and differences of them as

$$\begin{aligned}
 A^+ &\equiv a_1 + a_0, \\
 A^- &\equiv a_1 - a_0, \\
 J^+ &\equiv h(j_1 + j_0), \\
 J^- &\equiv h(j_1 - j_0), \\
 S^+ &\equiv h^2(s_1 + s_0), \\
 S^- &\equiv h^2(s_1 - s_0),
 \end{aligned} \tag{A.1}$$

where $h = (t_1 - t_0)/2$ and $a^{(k)}$ is the k th derivative of a . Coefficients of the interpolation polynomial at the midpoint $t = (t_0 + t_1)/2$ are

$$\begin{aligned}
 a_{1/2} &= \frac{1}{16}(8A^+ - 5J^- + S^+), \\
 hj_{1/2} &= \frac{1}{16}(15A^- - 7J^+ + S^-), \\
 \frac{h^2}{2}s_{1/2} &= \frac{1}{8}(3J^- - S^+), \\
 \frac{h^3}{6}a_{1/2}^{(3)} &= \frac{1}{8}(-5A^- + 5J^+ - S^-), \\
 \frac{h^4}{24}a_{1/2}^{(4)} &= \frac{1}{16}(-J^- + S^+), \\
 \frac{h^5}{120}a_{1/2}^{(5)} &= \frac{1}{16}(3A^- - 3J^+ + S^-).
 \end{aligned} \tag{A.2}$$

By shifting them to t_1 , we have derivatives for the next predictor or timestep criterion.

$$\begin{aligned}
 a_1^{(3)} &= a_{1/2}^{(3)} + ha_{1/2}^{(4)} + \frac{h^2}{2}a_{1/2}^{(5)}, \\
 a_1^{(4)} &= a_{1/2}^{(4)} + ha_{1/2}^{(5)}, \\
 a_1^{(5)} &= a_{1/2}^{(5)}.
 \end{aligned} \tag{A.3}$$

By integrating the even-order terms, we obtain the sixth-order corrector

$$v_1 - v_0 = h \left(A^+ - \frac{2}{5} J^- + \frac{1}{15} S^+ \right). \quad (\text{A.4})$$

A.2 Interpolation polynomial for the eighth-order integrator

The interpolation polynomial for the eighth-order integrator is constructed from (a_0, j_0, s_0, c_0) and (a_1, j_1, s_1, c_1) . Here c is crackle. Even-order coefficients are

$$\begin{pmatrix} a_{1/2} \\ \frac{h^2}{2} s_{1/2} \\ \frac{h^4}{24} a_{1/2}^{(4)} \\ \frac{h^6}{720} a_{1/2}^{(6)} \end{pmatrix} = \frac{1}{32} \begin{pmatrix} 16 & -11 & 3 & -1/3 \\ 0 & 15 & -7 & 1 \\ 0 & -5 & 5 & -1 \\ 0 & 1 & -1 & 1/3 \end{pmatrix} \begin{pmatrix} A^+ \\ J^- \\ S^+ \\ C^- \end{pmatrix}, \quad (\text{A.5})$$

and odd-order ones are

$$\begin{pmatrix} h j_{1/2} \\ \frac{h^3}{6} c_{1/2} \\ \frac{h^5}{120} a_{1/2}^{(5)} \\ \frac{h^7}{5040} a_{1/2}^{(7)} \end{pmatrix} = \frac{1}{32} \begin{pmatrix} 35 & -19 & 4 & -1/3 \\ -35 & 35 & -10 & 1 \\ 21 & -21 & 8 & -1 \\ -5 & 5 & -2 & 1/3 \end{pmatrix} \begin{pmatrix} A^- \\ J^+ \\ S^- \\ C^+ \end{pmatrix}, \quad (\text{A.6})$$

with

$$\begin{aligned} C^+ &\equiv h^3(c_1 + c_0), \\ C^- &\equiv h^3(c_1 - c_0). \end{aligned} \quad (\text{A.7})$$

The eighth-order corrector is

$$v_1 - v_0 = h \left(A^+ - \frac{3}{7} J^- + \frac{2}{21} S^+ - \frac{1}{105} C^- \right). \quad (\text{A.8})$$

References

Aarseth, J., S., 1903, MNRAS, 26, 223

- Aarseth, S. J. 1963, in *Multiple Time Scales*, ed. Brackbill and Cohen (Academic Press, New York), p. 377
- Aarseth, J., S., 2003, *Gravitational N-Body Simulations* (Cambridge Univ. Pr., Cambridge)
- Funato, Y., Makino, J., McMillan, S., & Hut, P. 1997, The Combination of Theory, Observations, and Simulation for the Dynamics of Stars and Star Clusters in the Galaxy, 23rd meeting of the IAU, Joint Discussion 15, 25 August 1997, Kyoto, Japan, meeting abstract., 15,
- Hut, P., & Makino, J. 2007, *The Art of Computational Science*, <http://www.artcompsci.org>
- Kokubo, E., Yoshinaga, K., & Makino, J. 1998, MNRAS, 297, 1067
- Kokubo, E., & Makino, J. 2004, PASJ, 56, 861
- Makino, J., 1991, ApJ 369, 200
- Makino, J., & Hut, P. 1988, apjs, 68, 833
- Makino, J. 1991b, PASJ, 43, 859
- Makino, J. & Aarseth, S. 1992, PASJ, 44, 141
- Makino, J., Taiji, M., Ebisuzaki, T., & Sugimoto, D. 1997, apj, 480, 432
- Makino, J., Fukushige, T., Koga, M., & Namura, K. 2003, PASJ, 55, 1163
- Makino, J., Hut, P., Kaplan, M., & Saygin, H. 2006, New Astronomy, 12, 124
- McMillan, S. L. W. 1986, in *The Use of Supercomputer in Stellar Dynamics*, ed. P. Hut & S. McMillan (New York: Springer), 156
- Warren, M. S., Salmon, J. K., Becker, D. J., Goda, M. P., & Sterling, T. 1997, In *The SC97 Proceedings*, CD-ROM. (IEEE, Los Alamitos, CA)